Proceedings of the ASME 2017 International Mechanical Engineering Congress and Exposition
IMECE2017
November 3-9, 2017, Tampa, Florida, USA

IMECE2017-71321

ATOMISTIC SIMULATION OF MIXED MODE FRACTURE IN VITREOUS SILICA

Simanta Lahkar
Department of Mechanical Engineering
BITS Pilani (Goa Campus)
Zuarinagar, Goa 403726
India

Subhas Ghosal
Department of Chemistry
BITS Pilani (Hyderabad Campus)
Hyderabad, Telangana 500078
India

Gaurav Singh*
Department of Mechanical Engineering
BITS Pilani (Goa Campus)
Zuarinagar, Goa 403726
India

ABSTRACT

In this work, molecular dynamics simulations have been used to study the brittle fracture behaviour of vitreous silica in mixed mode loading at room temperature. An implementation of the BKS potential with the coulombic term was used along with Lennard-Jones modification to model initial cristobalite. Ewald summation was used to obtain long-range coulombic contribution to the total potential energy of the system. A recipe (Huff et. al., Journal of Non-Crystalline Solids, 253, 133-142, 1999) was used to obtain the vitreous silica using a combination of different molecular dynamics runs which were done initially as NVT ensemble and at the end as NPT ensemble. Uniaxial tensile tests for uncracked specimen was carried out to validate the microscopic and macroscopic properties with that in the literature. Further, slit center cracks of different orientations were introduced in the vitreous silica and subjected to mixed mode loading by moving the boundaries slowly. Studies of mechanical behaviour were made to derive the variation of fracture stress and stiffness with the mode-mixity in amorphous solids.

NOMENCLATURE

β Crack inclination with respect to the loading
σ_β Overall stress for a sample with crack inclined at β
ε_β Overall strain for a sample with crack inclined at β
σ_β^{max} Maximum value of σ_β
E_β Stiffness of sample with β crack inclination
$E_{uncracked}$ Stiffness of uncracked sample

INTRODUCTION

Vitreous silica glass is used in high temperature mechanical systems (*e.g.* thermal protection system of reusable launch vehicles) as it has a very low thermal expansion [1]. Over time, various efforts have been made to mechanically characterize vitreous silica [2–7] which includes some tests in high temperature conditions. However, since the thermal protection systems have to operate in extreme conditions (as high as 1300°C) [8], experiments may not always be possible at such temperatures to derive mechanical properties (Young's modulus, Poissons ratio, mechanical strength, *etc*). An alternative to this limitation maybe to formulate the problem as that of a continuum finite thermoelasticity [9–11]. However, continuum approaches have not been proved to work at extremely high temperatures as the assumed non-linearity may not be valid.

Over the course of last two decades, advances in computational sciences have helped enable molecular dynamics (MD) simulations to model vitreous silica. MD simulation method is based on first principles and hence non-linear interactions and high temperature dependent properties can be estimated with more accuracy. A detailed account for the preparation of vitreous silica from the reported crystal structure [12] has been utilized to study mechanical behaviour [13–15]. The above quoted MD simulations are done at room temperature, only the tensile tests have been performed at extremely high temperatures [16]. Liquid silica under high pressures has also been studied through MD simulations [17]. The mechanical properties of amorphous silica has shown a strong size dependence at atomic the level [18]. Interestingly, deviations from the standard (MD) methods of prepa-

*Address all correspondence to this author.

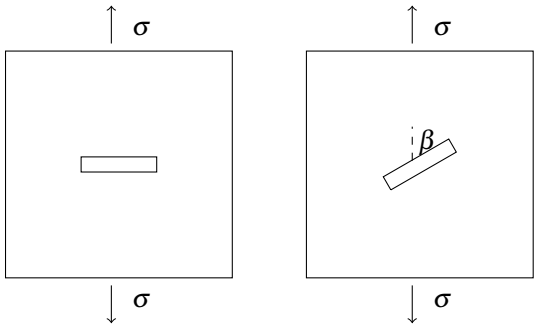

(a) Normal load (b) Mixed load

FIGURE 1: A CRACKED SOLID UNDER THE ACTION OF A UNIAXIAL LOAD.

rations have shown to change the properties of silica glass, *e.g.* a pressure quenching route results in increase in ductility [19].

A common problem in fracture mechanics has been to study the direction of crack growth for a given general loading as shown in Fig. 1. A consensus is lacking on account of multiple continuum-based criteria: maximum principal stress [20], minimum strain energy density [21], maximum strain energy release rate [22] *etc*. For small perturbations around pure normal loading, the maximum principal stress criterion has been argued to be enough [23], however, generally it is not valid for even the simple isotropic solids. An established criterion of crack growth may enable a better designing of product, for example, a control over the microstructure will enable a known macro crack growth path [24]. A lattice model for dynamic crack growth has been implemented in ANSYS to allow crack growth to choose its own direction [25]. For fracture at an atomic scale, the crack will grow straight ahead even for mixed loading for a pure crystal which has crack along the plane of weakness [26]. But, for complicated atomic systems earlier reports were unable to correctly identify a criterion for crack growth directions in mixed mode loadings [27–29]. The present work is directed towards addressing this larger issue, however, only the macroscopic mechanical response has been reported in the present work. In the following sections, a discussion on the preparation of vitreous silica will be followed by mixed-mode fracture simulation to note the overall fracture strength and stiffness of amorphous solids.

MODELLING

The simulations have been carried out using an atomistic model of vitreous silica which is prepared by quenching an initial cristobalite sample from high temperature. An initial specimen of high temperature cristobalite is prepared from reported crystal structure [30] consisting of 1200 silicon and 2400 oxygen atoms with dimensions $42.96\times35.8\times35.8$ Å^3. The interatomic interactions are modelled using *ab initio* BKS potential [31]. The BKS potential is modified with a steep short range Lennard-Jones term to prevent unphysical divergences at short distances between the atoms. Such modification was necessary for the current system as during the quenching process at high temperatures the interacting atoms can come very close to each other. The modified potential can be represented as

$$\phi_{ij} = \frac{q_i q_j}{r_{ij}} + A_{ij}\exp(-b_{ij}r_{ij}) - \frac{C_{ij}}{r_{ij}^6} + 4\varepsilon_{ij}\left[\frac{\sigma_{ij}}{r_{ij}}\right]^{24} - 4\varepsilon_{ij}\left[\frac{\sigma_{ij}}{r_{ij}}\right]^{6}$$

where, ϕ_{ij} is the potential energy for the interatomic separation r_{ij}. Other parameters, as reported in an earlier study [13], are listed in Tab. 1.

TABLE 1: POTENTIAL PARAMETERS FOR MD SIMULATIONS.

Interaction type	A_{ij} (eV)	b_{ij} (Å^{-1})	c_{ij}(eV/Å^6)	ε_{ij}(eV)	σ_{ij} (Å)
Si—O	18003.7572	4.8732	133.5381	1.12245×10^{-2}	1.31
O—O	1388.7730	2.76	175.0	3.5653×10^{-4}	2.2
Si—Si	-	-	-	12.6387	0.42

A cut-off of 8 Å was used along with Ewald summation [32] for rapid convergence of coulombic interactions over long interatomic distances to the total potential energy of the system. A standard velocity verlet scheme of integration [33], was used for solving the equations of motion for this simulation.

For the initial model, a minimization of the total energy of the system was performed, by relaxing the size of the box during the simulation. To get the optimum atomic coordinates corresponding to the particular potential the system was first relaxed. The system, thus obtained, was melted at 8000 K, and then stepwise quenching was activated towards achieving room temperature ($\sim$300 K) over a time duration of 212 ps. A method described in literature [12] had been used for this purpose. The final equilibration of the sample was carried out as NPT ensemble at zero pressure and 300K temperature for another 10 ps.

The vitreous silica glass model thus obtained had a mass density of 2.3 g/cc, slightly higher than the experimental value [2]. The radial distribution function (RDF) data and coordination number (CN) for the atoms was obtained for verifying the model. The first neighbour RDF for the Si-O bond, for the unstrained vitroues silica model, has a peak around $\sim$1.61 Å as shown in Fig. 2 (strain = 0.00). This value is in close agreement to the existing experimental data as discussed by Huff *et. al.* [12]. Further the average coordination number of Si and O atoms have been investigated and verified for unstrained vitreous silica model. For obtaining the coordination number of Si, average number of O

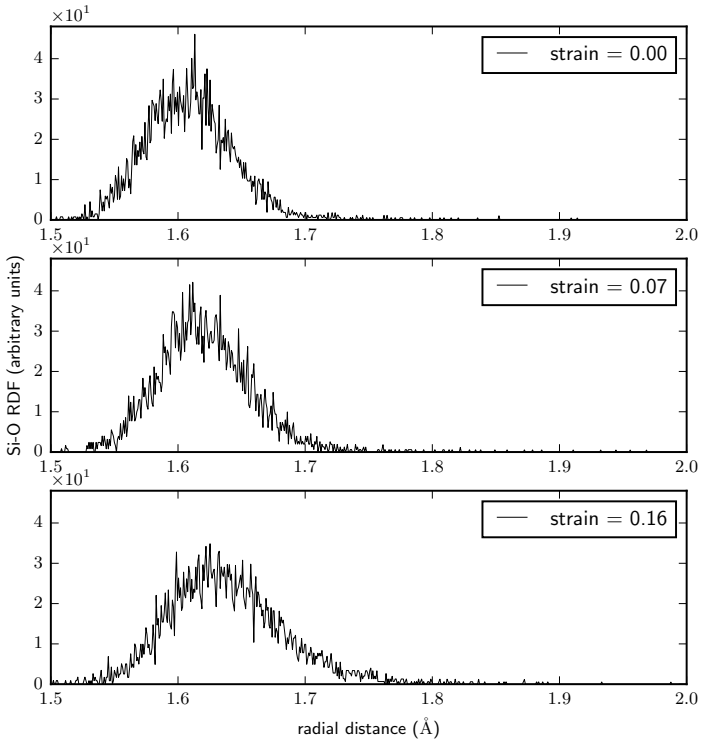

FIGURE 2: RADIAL DISTRIBUTION FUNCTION (RDF) IN THE ELASTIC REGION.

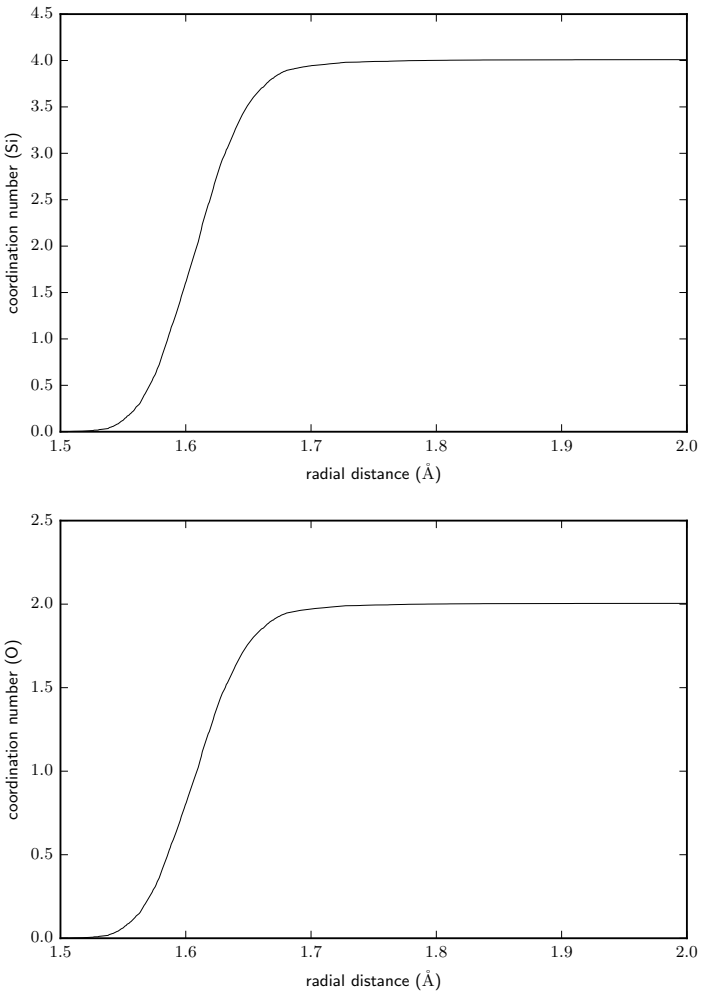

FIGURE 3: COORDINATION NUMBER VARIATION FOR SILICON AND OXYGEN IN VITREOUS SILICA

atoms within a given distance of a Si atom was plotted, and vice versa for O, as shown in Fig. 3 upper and lower panel, respectively. Two atoms are said to be coordinated if they are within 1.1 times the sum of the bond radii of the two atoms [12]. Considering the bond length to be 1.61 Å, as obtained from the RDF plot, we can observe from the plots that, corresponding to a distance of 1.77 Å, the average coordination number for Si and O in our model are in close agreement with the expected values of 4 and 2, respectively [12].

Further, tensile tests were carried out, based on the method described by Simmons *et. al.* [34], in which longitudinal strain was applied to the sample by increasing the length of the simulation box in the *x*-direction and remapping the *x*-coordinates of the atoms, keeping the lateral box boundaries fixed. Strain rates were varied from 0.1/ps to 0.005/ps and the stress response of the system were calculated using virial theorem [35]. Another tensile test was carried out with strain rate 0.01/ps in the *x*-direction, where zero pressure was maintained in lateral boundaries of the simulation box using Nosé-Hoover barostat under NPT conditions [36]. The temperature for the tensile tests were maintained at 300 K using Nosé-Hoover thermostat [37, 38].

The stress-strain curve, obtained from the tensile tests at different strain rates, are shown in Fig. 4 for the prepared model in NVT ensemble. It can be clearly seen that each curve has 4 distinct regions as described in earlier work [34]. This maybe seen as a macroscopic validation of the model. To further validate the suitability of the model for such tests, the RDF plots at different strain values for a representative strain rate of 0.01/ps are shown in Fig. 2. It maybe observed that the Si-O RDF peak shifts to larger separation distances with increase in strain in the elastic region (until strain≈0.16 in Fig. 4). With further increase in strain, in the yield region (from strain between 0.16 and 0.22 in Fig. 4), the Si O peak remains fairly unchanged, as observed in Fig. 5. Finally at larger strains (beyond 0.22 in Fig. 4), after fracture has occured, the peak shifts back to 1.61 Å as shown in Fig. 6. These observations agree with that in the earlier work of Muralidharan *et. al.* [13].

The average stiffness (as a slope of the linear elastic region

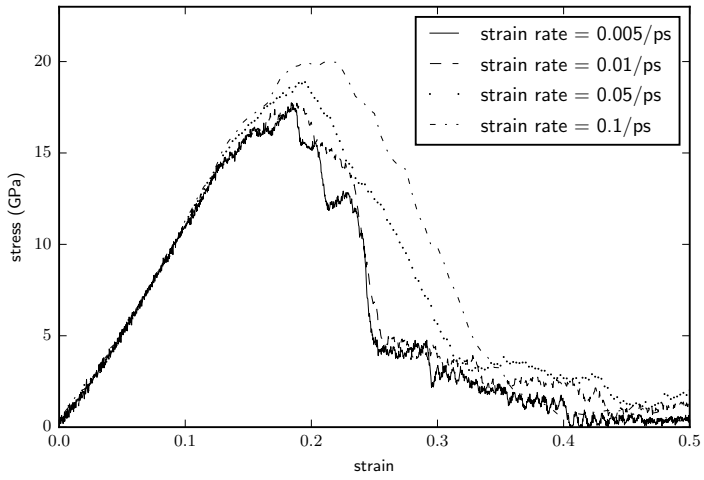

FIGURE 4: MECHANICAL RESPONSE OF VITREOUS SILICA UNDER REMOTE QUASI-STATIC LOADING.

in Fig. 4) and the fracture stress (as a maximum stress in Fig. 4), obtained at different strain rates for the NVT tensile tests are tabulated in Tab. 2. From these values and the plots, it is observed that for the initial elastic region, the variation in stress with increase in strain in the model is almost same for different strain rates. However, the fracture stress increases with increase in the strain rate. These data from the NVT tensile tests on our prepared vitreous silica model agree very well with those obtained in the earlier work [13].

TABLE 2: FRACTURE STRESS AND STIFFNESS OF VITREOUS SILICA AT DIFFERENT STRAIN RATES

Strain rate (/ps)	Fracture stress (GPa)	Stiffness (GPa)
0.005	17.520	112.450
0.010	17.730	113.320
0.050	18.870	114.620
0.100	20.040	116.210

From the tensile test carried out on the uncraked model in an NPT ensemble, the stiffness in the elastic region, maximum tensile strength and Poisson's ratio were calculated as 96.34 GPa, 16.42 GPa, and 0.29 GPa, respectively. The stress-strain curve for this test has been plotted in Fig. 7, along with the stress-strain curve of NVT tensile test, with strain rate = 0.01/ps, for comparison. The stiffness (Young's modulus) from the NPT test is lower than in the NVT tests. Another prominent difference

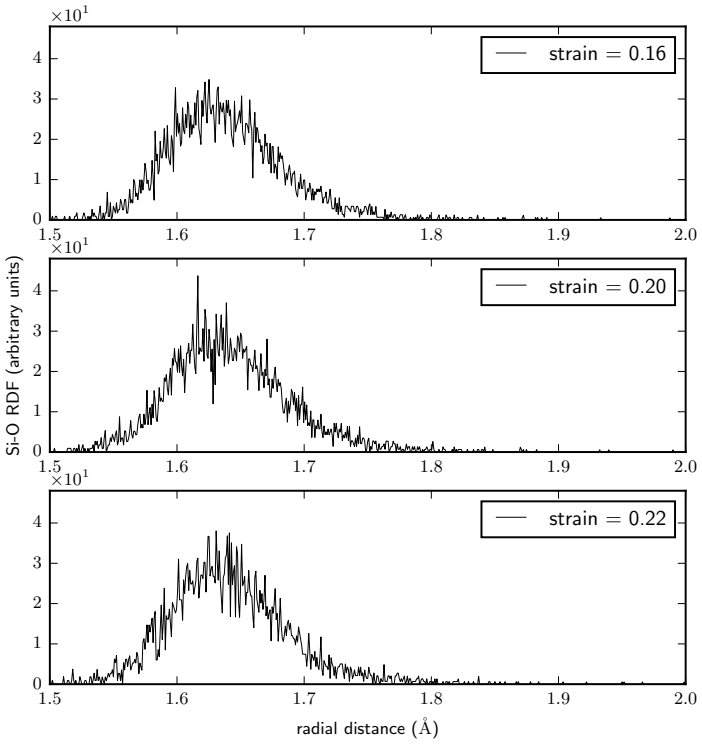

FIGURE 5: RDF IN THE YIELD REGION.

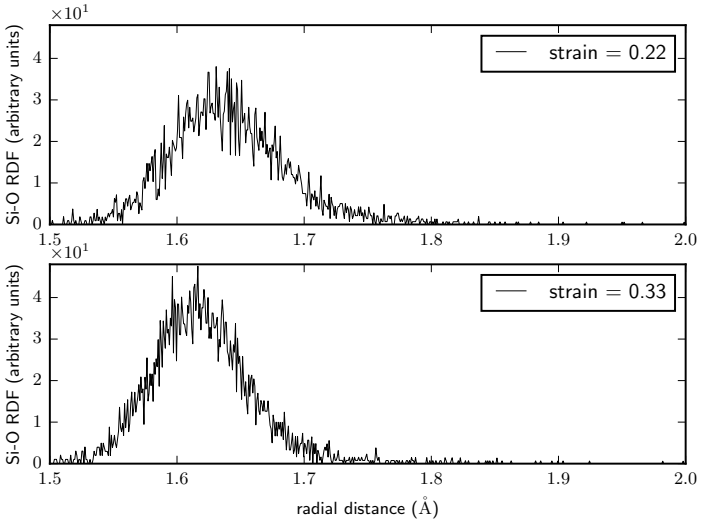

FIGURE 6: RDF BEYOND THE YIELD REGION.

is that the sample shows ductile nature under NPT conditions. A similar behaviour has been obtained in literature [18]. Such observations were also made in continuum based methods [39] for small element sizes. The aforementioned results prove that the vitreous silica has indeed been correctly modeled, which will

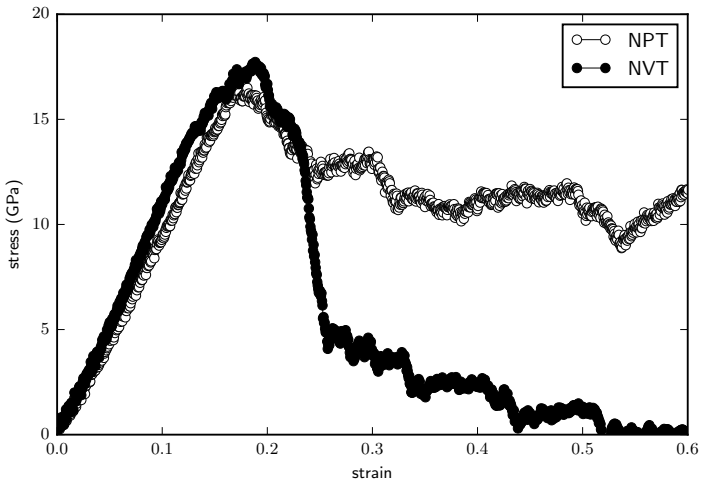

FIGURE 7: MECHANICAL RESPONSE OF VITREOUS SILICA UNDER REMOTE QUASI-STATIC LOADING

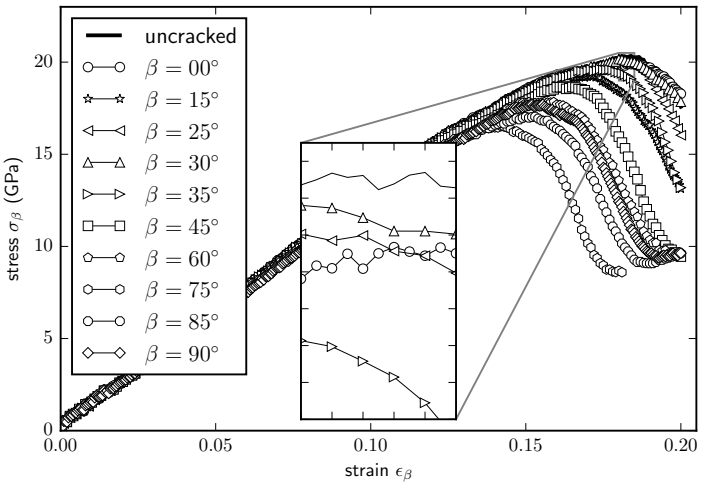

FIGURE 8: MECHANICAL RESPONSE OF CRACKED VITREOUS SILICA UNDER REMOTE QUASI-STATIC LOADING.

now be used to effectively model and study fracture behaviour under mixed mode loading.

The crack model used to study mixed-mode fracture in vitreous silica (prepared according to the aforementioned discussion) in the present study is based on non-amorphous graphene [29]. The length$\times$width$\times$thickness of the samples were $125 \times 105 \times 35$ Å^3 with a slit center crack of 20 Å. The slit crack was made simply by breaking the bonds between atoms across the intended crack without any removal of atoms. The bottom edge was fixed, and the model pulled along its length as the top edge was deformed at a constant strain rate of 0.01/ps. Atoms in the narrow boundary regions along the four lateral edges were forced to a zero planar force and velocity every deformation step/ time step. Thus the sides of the model were constrained along the width and length and the model boundaries continued to remain in the deformed position during the time integration step after deformation was applied. The temperature of the sample was maintained using a Berendsen thermostat [40] and the simulation was done under NVE ensemble. Though the cracked sample dimensions and loading conditions were same in all the simulations, different crack inclinations β were created at $00°, 15°, 30°, 45°, 60°, 75°$ and $90°$. The stress strain behaviour of the samples were recorded using the virial stress calculations [41] for the whole specimen at discrete timesteps. Results of this study are discussed in the next section.

RESULTS

The stress-strain response of the cracked vitreous silica samples have been shown in Fig. 8. All samples show a linear behaviour at low strains and soften after achieving the fracture stress. The zoomed-inset shows the fracture (peak) stress region of a few cases. Since the monotonity in the variation was observed to break at $\beta = 30°$ and $\beta = 90°$, additional tests were done for samples with a $\beta = 25°, 35°$ and $\beta = 85°$.

The fracture stress identifies the state when the crack grows uncontrollably (fracture). The samples are visually observed to fracture at this stress. The normalized fracture stress of different inclinations of cracks in vitreous silica is shown in Fig. 9. The fracture stress has been calculated as the maximum stress of the stress-strain variation in Fig. 8. It maybe observed that, other than small and large crack inclinations, the fracture stress decreases with an increasing crack inclination. This is qualitatively consistent with the commonly used linear elasticity based criteria of crack growth like minimum strain energy density or maximum tensile.

The normalized stiffness (Young's modulus) of different inclinations of cracks in vitreous silica is shown in Fig. 10. The stiffness has been calculated as the slope of the linear region of the stress-strain variation in Fig. 8. It maybe observed that, other than small and large crack inclinations, the stiffness decreases with an increasing crack inclination.

CONCLUSIONS

In the present work, mixed mode fracture in vitreous silica has been atomistically modelled to study the variation of fracture stress and stiffness (Young's modulus) with the mode-mixity (crack inclination). The major trends were consistent with the continuum-based theories, however deviations were observed. These maybe attributed to the fact that the continuum-based the-

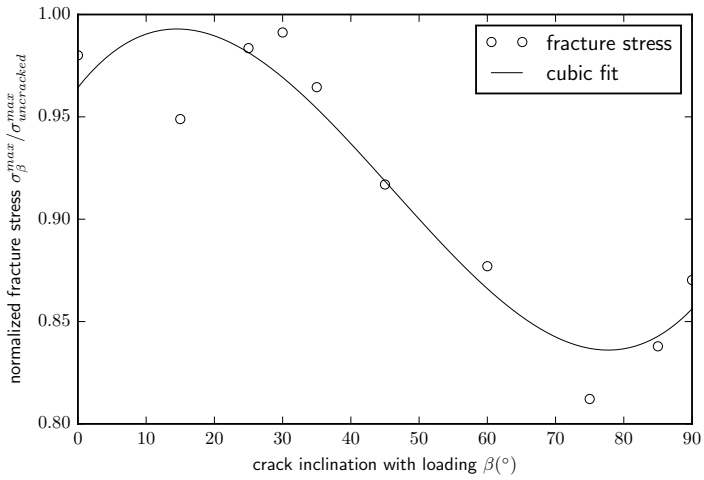

FIGURE 9: VARIATION OF FRACTURE STRESS OF VITREOUS SILICA WITH CRACK INCLINATION.

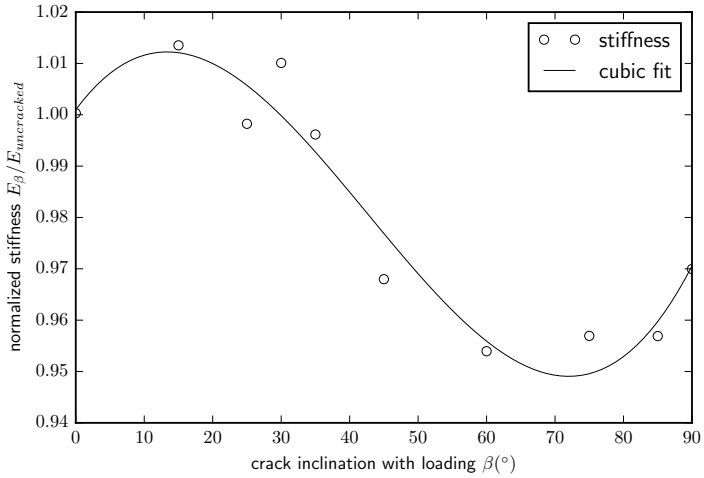

FIGURE 10: VARIATION OF EFFECTIVE STIFFNESS OF VITREOUS SILICA WITH CRACK INCLINATION.

ories are based on linear elasticity while the simulation in the present work makes no such simplification. The present work is intended to be extended at two levels - firstly, to be able to correctly predict crack growth direction using the void formation near crack and secondly, predict fracture behaviour at high temperature aerospace applications.

ACKNOWLEDGEMENTS

SG thanks DST FIST grant SR/FST/CSI-240/2012 for computational facilities.

REFERENCES

[1] Paté-Cornell, E., and Fischbeck, P. S., 1993. "Probabilistic risk analysis and risk-based priority scale for the tiles of the space shuttle". *Reliability Engineering & System Safety,* ***40***(3), pp. 221 – 238.

[2] Brücker, R., 1970. "Properties and structure of vitreous silica. I". *Journal of Non-Crystalline Solids,* ***5***(2), pp. 123 – 175.

[3] McSkimin, H. J., 1953. "Measurement of elastic constants at low temperatures by means of ultrasonic wavesdata for silicon and germanium single crystals, and for fused silica". *Journal of Applied Physics,* ***24***(8), pp. 988–997.

[4] Spinner, S., and Cleek, G. W., 1960. "Temperature dependence of young's modulus of vitreous germania and silica". *Journal of Applied Physics,* ***31***(8), pp. 1407–1410.

[5] Elmer, T. H., 1991. *Porous and reconstructed glasses*, Vol. 4 of *Engineered Materials Handbook*. ASM International.

[6] Shelby, J. E., 2004. "Density of vitreous silica". *Journal of Non-Crystalline Solids,* ***349***, pp. 331 – 336. Glass Science for High Technology. 16th University Conference on Glass Science.

[7] Yue, Y., and Zheng, K., 2014. "Strong strain rate effect on the plasticity of amorphous silica nanowires". *Applied Physics Letters,* ***104***(23), p. 231906.

[8] Moo Y. Lee, John H. Hofer, D. R. B., and Hardy, R. D., 2005. "Validity of linear elasticity in the crack-tip region of ideal brittle solids". *Department of Energy,United States.*

[9] Maneschy, C., 1994. "Thermoelastic analysis of a mooney-rivlin slab under inhomogeneous shearing". *International Journal of Solids and Structures,* ***31***(3), pp. 317 – 327.

[10] Rajagopal, K. R., 1995. "Boundary layers in finite thermoelasticity". *Journal of Elasticity,* ***36***(3), pp. 271–301.

[11] Bilgili, E., Bernstein, B., and Arastoopour, H., 2001. "Inhomogeneous shearing deformation of a rubber-like slab within the context of finite thermoelasticity with entropic origin for the stress". *International Journal of Non-Linear Mechanics,* ***36***(6), pp. 887 – 900.

[12] Huff, N. T., Demiralp, E., Çagin, T., and Goddard III, W. A., 1999. "Factors affecting molecular dynamics simulated vitreous silica structures". *Journal of non-crystalline solids,* ***253***(1), pp. 133–142.

[13] Muralidharan, K., Simmons, J., Deymier, P., and Runge, K., 2005. "Molecular dynamics studies of brittle fracture in vitreous silica: review and recent progress". *Journal of non-crystalline solids,* ***351***(18), pp. 1532–1542.

[14] Muralidharan, K., Oh, K.-D., Deymier, P. A., Runge, K., and Simmons, J. H., 2007. "Molecular dynamics simulations of atomic-level brittle fracture mechanisms in amorphous silica". *Journal of Materials Science,* ***42***(12), mar, pp. 4159–4169.

[15] Pedone, A., Malavasi, G., Menziani, M. C., Segre, U., and

Cormack, A. N., 2008. "Molecular dynamics studies of stressstrain behavior of silica glass under a tensile load". *Chemistry of Materials,* ***20***(13), pp. 4356–4366.

[16] Zhang, Y., Zhang, D. H., Li, Z. P., Ding, Y. F., and Zhang, F. W., 2007. "Molecular dynamics study of the structure in vitreous silica with compass force field at elevated temperatures". In Progress in Light Metals, Aerospace Materials and Superconductors, Vol. 546 of *Materials Science Forum*, Trans Tech Publications, pp. 2189–2193.

[17] Horbach, J., 2008. "Molecular dynamics computer simulation of amorphous silica under high pressure". *Journal of Physics: Condensed Matter,* ***20***(24), p. 244118.

[18] Yuan, F., and Huang, L., 2012. "Molecular dynamics simulation of amorphous silica under uniaxial tension: From bulk to nanowire". *Journal of Non-Crystalline Solids,* ***358***(24), pp. 3481–3487.

[19] Yuan, F., and Huang, L., 2014. "Brittle to ductile transition in densified silica glass". *Scientific Reports,* ***4***(1), May.

[20] Erdogan, F., and Sih, G. C., 1963. "On the crack extension in plates under plane loading and transverse shear". *Journal of Basic Engineering,* ***85***(4), p. 519.

[21] Sih, G. C., 1974. "Strain-energy-density factor applied to mixed mode crack problems". *International Journal of Fracture,* ***10***(3), sep, pp. 305–321.

[22] Strifors, H. C., 1974. "A generalized force measure of conditions at crack tips". *International Journal of Solids and Structures,* ***10***(12), pp. 1389 – 1404.

[23] Ohtsuka, K., 2002. "Comparison of criteria on the direction of crack extension". *Journal of Computational and Applied Mathematics,* ***149***(1), pp. 335 – 339. Scientific and Engineering Computations for the 21st Century - Me thodologies and Applications Proceedings of the 15th Toyota Conference.

[24] Srivastava, A., Osovski, S., and Needleman, A., 2017. "Engineering the crack path by controlling the microstructure". *Journal of the Mechanics and Physics of Solids,* ***100***, pp. 1 – 20.

[25] Trevisan, A., Borzi, G. P., Movchan, N. V., Movchan, A. B., and Brun, M., 2016. "Thermal shock driven fracture in a structured solid: dynamic crack growth and nucleation". *International Journal of Fracture,* ***202***(2), jun, pp. 167–177.

[26] Singh, G., Kermode, J. R., Vita, A. D., and Zimmerman, R. W., 2014. "Validity of linear elasticity in the crack-tip region of ideal brittle solids". *International Journal of Fracture,* ***189***(1), jul, pp. 103–110.

[27] Zhou, X., Zimmerman, J., Jr., E. R., and Moody, N., 2008. "Molecular dynamics simulation based cohesive surface representation of mixed mode fracture". *Mechanics of Materials,* ***40***(10), pp. 832 – 845.

[28] Paliwal, B., and Cherkaoui, M., 2013. "An improved atomistic simulation based mixed-mode cohesive zone law considering non-planar crack growth". *International Journal of Solids and Structures,* ***50***(2021), pp. 3346 – 3360.

[29] Datta, D., Nadimpalli, S. P., Li, Y., and Shenoy, V. B., 2015. "Effect of crack length and orientation on the mixed-mode fracture behavior of graphene". *Extreme Mechanics Letters,* ***5***, pp. 10 – 17.

[30] Barth, T. F. W., 1932. "The cristobalite structures". *Am J Sci,* ***23***, Apr, pp. 350–356.

[31] van Beest, B. W. H., Kramer, G. J., and van Santen, R. A., 1990. "Force fields for silicas and aluminophosphates based on ab initio calculations". *Phys. Rev. Lett.,* ***64***, Apr, pp. 1955–1958.

[32] Wells, B. A., and Chaffee, A. L., 2015. "Ewald summation for molecular simulations". *Journal of Chemical Theory and Computation,* ***11***(8), pp. 3684–3695. PMID: 26574452.

[33] Swope, W. C., Andersen, H. C., Berens, P. H., and Wilson, K. R., 1982. "A computer simulation method for the calculation of equilibrium constants for the formation of physical clusters of molecules: Application to small water clusters". *The Journal of Chemical Physics,* ***76***(1), pp. 637–649.

[34] Ochoa, R., and Simmons, J. H., 1985. "High strain rate effects on the structure of a simulated silica glass". *Journal of Non-Crystalline Solids,* ***75***(1), pp. 413 – 418.

[35] M. P. Allen, D. J. T., 1989. *Computer simulation of liquids*. Oxford University Press, USA.

[36] Tuckerman, M. E., and Martyna, G. J., 2000. "Understanding modern molecular dynamics: techniques and applications". *The Journal of Physical Chemistry B,* ***104***(2), pp. 159–178.

[37] Hoover, W. G., 1985. "Canonical dynamics: Equilibrium phase-space distributions". *Phys. Rev. A,* ***31***, Mar, pp. 1695–1697.

[38] Nosé, S., 1984. "A molecular dynamics method for simulations in the canonical ensemble". *Molecular Physics,* ***52***(2), pp. 255–268.

[39] Bargmann, S., Xiao, T., and Klusemann, B., 2014. "Computational modelling of submicron-sized metallic glasses". *Philosophical Magazine,* ***94***(1), pp. 1–19.

[40] Berendsen, H. J. C., Postma, J. P. M., van Gunsteren, W. F., DiNola, A., and Haak, J. R., 1984. "Molecular dynamics with coupling to an external bath". *The Journal of Chemical Physics,* ***81***(8), pp. 3684–3690.

[41] Pei, Q., Zhang, Y., and Shenoy, V., 2010. "A molecular dynamics study of the mechanical properties of hydrogen functionalized graphene". *Carbon,* ***48***(3), pp. 898 – 904.